3-1-2015

The Dust Geometric Distribution in Seyfert 1 and Seyfert 2 Galaxies, Isolated and in Interaction

S. Mendoza-Castrejón
Universidad Nacional Autónoma de México, Mexico

D. Dultzin
Universidad Nacional Autónoma de México, Mexico

Y. Krongold
Universidad Nacional Autónoma de México, Mexico

J. J. González
Universidad Nacional Autónoma de México, Mexico

Moshe Elitzur
University of Kentucky, moshe@pa.uky.edu

Monthly Notices
of the
ROYAL ASTRONOMICAL SOCIETY

MNRAS **447,** 2437–2444 (2015) doi:10.1093/mnras/stu2566

The dust geometric distribution in Seyfert 1 and Seyfert 2 galaxies, isolated and in interaction

S. Mendoza-Castrejón,[1]★ D. Dultzin,[1] Y. Krongold,[1] J. J. González[1] and M. Elitzur[2]

[1]*Instituto de Astronomía, Universidad Nacional Autónoma de México, Apartado Postal 70-264, México, DF 04510, México*
[2]*Departament of Physics and Astronomy, University of Kentucky, Lexington, KY 40506, USA*

Accepted 2014 December 2. Received 2014 November 7; in original form 2014 August 11

ABSTRACT

We analyse the mid-infrared (MIR) spectra of 39 Seyfert galaxies observed with the Infrared Spectrograph (IRS) on board the *Spitzer Space Telescope*. Our sample consists of 19 Seyfert type 1 (Sy1) galaxies, three intermediate Seyfert galaxies and 17 type 2 Seyfert (Sy2) galaxies in the nearby Universe. This sample was extracted from a larger sample, the circumgalactic environment of which was studied in a previous work by Dultzin-Hacyan et al., who found that Sy2 objects are in interaction more frequently than normal galaxies, while Sy1s are not. In this article, we study the silicate dust distribution that dominates the mid-infrared (MIR) spectra. This dust produces spectral features at 10 and 18 μm that are sensitive to the clumpiness of the dust. We measure the strength of the emission or absorption of the silicate features to find whether there is a correlation between the clumpiness of the circumnuclear dust and the active galactic nucleus (AGN) type and incidence of companions. All isolated Sy1 galaxies have clumpy dust distributions, whereas Sy1s with a close companion can have either clumpy or smooth distributions. In the case of Sy2 galaxies, those with one or more companions have mostly smooth dust distributions, whereas isolated Sy2s may have clumpy or smoothly distributed dust. Our result is at odds with the simplest formulation of the unified scheme for Seyferts and supports an evolutionary sequence where the influence of an interaction triggers a type 2 AGN, which evolves into a type 1.

Key words: dust, extinction – galaxies: nuclei – galaxies: Seyfert.

1 INTRODUCTION

The unified scheme for active galactic nuclei (AGNs), currently the dominant paradigm, postulates that the diverse spectral properties that determine the diverse types of AGN correspond to different orientations between the circumnuclear dust torus surrounding the accretion disc and the line of sight (Antonucci 1993). According to this scheme, the only difference between type 1 and 2 AGNs is that the central engine of an AGN, including the broad-line region (BLR), is completely obscured when viewed along directions intercepted by the dusty torus and it is then classified as a type 2. On the other hand, when the line of sight to the central engine is clear we see a type 1 AGN. This scheme received strong support from the fact that broad lines were revealed in the spectra of Seyfert 2 (Sy2) galaxies in polarized light (Antonucci & Miller 1985). However, later on it was found that hidden BLRs are only observable in 50 per cent of Sy2 galaxies (Tran 2001, 2003), indicating the possible existence of *pure* type 2 objects (Gu, Maiolino & Dultzin-Hacyan 2001). These objects may intrinsically lack a BLR, which can be explained in terms of a very low accretion rate (Nicastro 2000; Elitzur 2008) or may be due to obscuration effects (Shu, Wang & Jiang 2008). Indeed, observational evidence suggests that Sy2s with polarized broad lines are more easily related to truly obscured Seyfert 1 (Sy1) nuclei, while *pure* Sy2s preferentially host weak AGNs. There is also evidence of non-obscured Seyfert 2 galaxies in the X-ray region (Bianchi et al. 2008; Brightman & Nandra 2008).

There are early works showing that Sy1 and Sy2 galaxies have different intrinsic properties in different wavebands (Dultzin-Hacyan & Benitez 1994; Dultzin-Hacyan & Ruano 1996). For example, optical studies suggest that Sy2 galaxies exhibit circumnuclear star-forming regions more frequently than Sy1 galaxies (Gonzalez-Delgado & Perez 1993; Gu et al. 2001); similar trends were found from IR studies (Maiolino & Rieke 1995; Maiolino et al. 1997). Also, Cid Fernandes et al. (2001) found that 50 per cent of Sy2 galaxies exhibit an intense starburst (SB). Recent results that compare near-infrared (NIR) with hard X-ray luminosities suggest that this difference is clear-cut only at low luminosities (Castro et al. 2014). Other studies, however, claim that there is no significant difference between type 1 and type 2 galaxies regarding star formation activity (Imanishi & Wada 2004).

With respect to the circumgalactic environment, the lack of type 1 AGNs in isolated pairs of galaxies (González et al. 2008) and in compact groups (Martínez et al. 2008; Bitsakis et al. 2010) is

★ E-mail: smendoza@astro.unam.mx

also in disagreement with the simplest formulation of the unified scheme. Furthermore, it has been shown that Sy2 galaxies are in interaction with similar mass close neighbours more often than normal galaxies, while Sy1s are not (Dultzin-Hacyan et al. 1999). It has also been shown that the frequency of interactions for Sy2s and starburst galaxies is similar (Krongold, Dultzin-Hacyan & Marziani 2002). More recent studies support this finding with observations that take into account the radial velocities of the neighbouring galaxies (Koulouridis et al. 2006a,b).

Despite the fact that the role of interactions in inducing activity is still an open issue (Koulouridis et al. 2006a,b, 2013), the above studies support a possible evolution of activity that follows the path: interactions → enhanced star formation → type II AGN → type I AGN (e.g. Krongold et al. 2002, 2003). This evolutionary sequence explains the differences between type 1 and type 2 AGNs, while at the same time being consistent with the unified scheme as a particular stage of the evolution.

In order to understand the physics of AGNs, a key issue is the nature of the obscuring medium surrounding the active nucleus. A key ingredient of the obscuring medium is thought to be a dusty torus on a parsec (pc) scale consisting of dusty clouds that are individually optically thick (Krolik & Begelman 1988). This dust in the torus reprocesses the radiation from the central engine to emerge at mid-infrared (MIR) wavelengths. The MIR spectral energy distribution (SED) is determined by the dust geometric distribution, the dust composition and the dust density distribution of the torus. Several studies have modelled the toroidal dust structure with the aim of comparing it with the observable properties. Early modelling work assumed smooth dust models (e.g. Pier & Krolik 1992, 1993; Granato & Danese 1994; Efstathiou & Rowan-Robinson 1995). More recently, several works suggested the existence of a clumpy torus (e.g. Krolik & Begelman 1988; Rowan-Robinson 1995; Nenkova, Ivezić & Elitzur 2002; Thompson et al. 2009). In particular, Nenkova et al. (2008a,b) have developed a formalism to calculate the SED of the clumpy structure.

The MIR spectra of galaxies is dominated by dust emission. Silicates, a major constituent of astronomical dust, reveal their presence through the spectral features at 10 and 18 μm. The stronger 10-μm silicate features originates from an SiO-stretching mode and the 18-μm silicate features from an SiO-bending mode (Knacke & Thomson 1973). Sirocky et al. (2008) have shown that the comparison of both silicate features is a reliable diagnostic of the dust chemistry and dust geometry around the AGN, distinguishing between smooth and clumpy distributions.

The aim of our article is to find a possible correlation between clumpiness of the circumnuclear dust distribution and AGN type and interaction incidence.

2 THE SAMPLE

The sample of Seyfert galaxies used for this study consists of 19 Sy1 galaxies, three intermediate Seyfert galaxies, and 17 Sy2 galaxies. We selected a subsample from Dultzin-Hacyan et al. (1999), which has been observed by the Infrared Spectrograph on board the *Spitzer* Space Telescope (Werner et al. 2004; Houck et al. 2004). The data we have used were obtained from different *Spitzer* programmes that have different observational goals. Therefore, our sample is not biased towards any particular type of objects with unique characteristics that may affect our conclusions. In Table 1, we present our sample and identify the original *Spitzer* programme from which the data were taken. The sample by Dultzin-Hacyan et al. (1999) was obtained from the catalogue of Lipovetsky, Neizvestny & Neizvestnaya (1988) and consists of 72 Sy1 galaxies (redshift $0.007 \leq z \leq 0.034$) and 60 Sy2 galaxies ($0.007 \leq z \leq 0.020$). The $V/V_{\rm max}$ test shows that the sample is complete to a level of 92 per cent. In order to avoid Galactic extinction, the objects were selected at high Galactic latitude, $b \geq 40^{\circ}$. For more details see Dultzin-Hacyan et al. (1999). In this study, the close environment of the galaxies was examined (within $\lesssim$100 kpc of the projected distance). It was found that the sample of Seyfert 2 galaxies shows an excess of large neighbours ($D_n \geq 10$ kpc) with respect to non-active galaxies, whereas that of Seyfert 1 galaxies does not. The distance distribution of Sy1s is somewhat larger than that of Sy2s. However, the cut-off magnitude used to select similar-mass companions does not bias the selection. We do not consider faint companions. This result was confirmed in a three-dimensional study by Koulouridis et al. (2006a,b). In order to distinguish between physical and projected companions, these authors used a radial velocity separation criterion of $\delta v \lesssim 600\,{\rm km\,s^{-1}}$.

Notice that, for the purpose of studying the environment, in these articles the few intermediate Seyfert galaxies were considered as type 1 or type 2 (those of type 1.5 or lower were included in the Sy1 sample and those with type 1.8 or 1.9 in the Sy2 sample). While the interpretation of intermediate Seyferts of 1.5 or lower is straightforward, as the broad component is strong, in the case of 1.8–1.9 objects their nature is more elusive. Their spectra may arise from a clear view of an intrinsically weak broad-line emission. If this is the case, these very weak broad-line objects would represent the link between type 1 AGNs and *pure* type 2 objects. However, their emission could also reflect scattered radiation from an obscured BLR with standard broad-line emission. In this case, they are type 2 objects. The only way to break this degeneracy is through separate observations to determine the obscuration of the nucleus and/or the line polarization.

Dultzin-Hacyan et al. (1999) estimated the fraction of interacting objects in their samples, which are only projections in the sky using statistical arguments, assuming a Poisson distribution for the field density. While this method is seen to be effective, it does not provide an exact identification of the bona fide physical companions. In order to avoid projected pairs of galaxies in our analysis, in this work we used the Sloan Digital Sky Survey (SDSS) and the NASA/IPAC Extragalactic Database (NED) to search for the nearest neighbours of each Seyfert within a projected radius of 100 h^{-1} kpc, a radial velocity separation $\delta v \lesssim 600\,{\rm km\,s^{-1}}$ and a magnitude limit of $m_B \sim 18.5$. The choice of 100 kpc was justified, as in Dultzin-Hacyan et al. (1999) it was clear that only this close environment was relevant (see their fig. 1). A radial velocity difference $\delta v \lesssim 600\,{\rm km\,s^{-1}}$ was chosen, as it is roughly the mean galaxy pairwise velocity of the Center for Astrophysics Galaxy Catalog (CfA2) as well as the Southern Sky Redshift Survey (SSRS); we note that this difference is about twice the mean pairwise galaxy velocity when clusters of galaxies are excluded (Marzke et al. 1995). This is the same procedure used by Koulouridis et al. (2006a,b), who also carried out their own survey searching for faint physical companions. Our independent search yields results fully consistent with those of these authors.

In addition to our search for physical companions, we also searched for evidence of past mergers in isolated galaxies, using both the literature and direct inspection over the SDSS images (searching for disturbed morphology). Seyfert 1 galaxy NGC 2782 was the only isolated object that showed a highly disturbed morphology, revealing a merger remnant (Torres-Flores et al. 2012, and reference there in). For this reason, we included this object in the sample of interacting Seyfert 1 galaxies. We also verified the

Table 1. Sample of Seyfert galaxies.

Name	*Spitzer* PID	RA (J2000.0)	Dec.(J2000.0)	m_B	z	Type	Environment
Mrk 590	30572	02 14 34.7	01 13 57	13.81	0.02700	Sy1	Interacting
ESO 548−G81	30745	03 42 03.0	−21 14 25	12.92	0.01148	Sy1	Isolated
NGC 2782	24	09 14 05.6	40 06 54	12.66	0.00854	Sy1	Interacting
1H1142−178	50588	11 45 40.4	−18 27 16	14.70	0.03295	Sy1	Interacting
Mrk 42	30715	11 53 42.1	46 12 42	15.20	0.02469	Sy1	Isolated
UGC 7064	3374	12 04 43.6	31 10 37	15.50	0.01341	Sy1	Interacting
NGC 4235	40936	12 17 09.8	07 11 28	13.20	0.00804	Sy1	Isolated
Mrk 50	50588	12 23 24.1	02 40 44	15.17	0.02300	Sy1	Isolated
IISZ10	20142	13 10 00.0	−10 51 00	15.55	0.03426	Sy1	Isolated
NGC 5077	30256	13 19 31.4	−12 39 24	14.00	0.01341	Sy1	Interacting
UM 614	50588	13 49 00.0	02 20 00	15.70	0.0327	Sy1	Isolated
Mrk 279	666	13 53 03.2	69 18 28	14.50	0.03025	Sy1	Interacting
NGC 5548	30572	14 17 59.5	25 08 09	13.10	0.01717	Sy1	Isolated
Mrk 290	20142	15 35 52.1	57 54 06	15.50	0.03062	Sy1	Isolated
NGC 7172	30572	22 02 02.1	−31 52 11	12.95	0.00859	Sy1	Interacting
Mrk 915	50588	22 36 46.6	−12 32 44	14.82	0.02391	Sy1	Interacting
UGC 12138	3374	22 40 17.0	08 03 12	14.64	0.01718	Sy1	Interacting
NGC 7469	14	23 03 15.5	08 52 24	13.00	0.01618	Sy1	Interacting
NGC 7603	3374	23 18 56.6	00 18 10	14.01	0.02900	Sy1	Interacting
Mrk 744	3374	11 39 42.8	31 54 33	13.50	0.00910	Sy1.8	Interacting
MCG –03–34–064	30323	13 22 24.2	−16 43 44	14.64	0.01718	Sy1.8	Interacting
UGC 1395	3374	01 55 21.9	06 36 45	14.00	0.01726	Sy1.9	Isolated
NGC 0454	50588	01 12 00.0	−55 39 00	14.0	0.01212	Sy2	Interacting
NGC 526A	30572	01 23 54.5	−53 03 54	14.66	0.01910	Sy2	Interacting
Mrk 573	50094	01 43 57.6	02 21 01	14.07	0.01658	Sy2	Isolated
NGC 788	30745	02 01 14.4	−06 49 30	14.87	0.01795	Sy2	Isolated
IC 1816	50588	02 31 51.2	−36 40 14	13.50	0.01360	Sy2	Isolated
ESO 417−G06	50588	02 56 21.5	−32 11 05	13.87	0.01105	Sy2	Interacting
NGC 1358	40936	03 33 39.6	−05 05 18	15.10	0.02066	Sy2	Interacting
NGC 4939	30572	13 04 14.0	−10 20 25	11.99	0.01040	Sy2	Isolated
NGC 5347	30572	13 53 17.8	33 29 24	13.18	0.00796	Sy2	Isolated
NGC 5427	3247	14 03 25.6	−06 01 53	11.93	0.00870	Sy2	Interacting
NGC 5506	86	14 13 14.6	−03 12 29	13.37	0.00585	Sy2	Interacting
Mrk 686	30773	14 37 22.1	36 34 01	13.90	0.01409	Sy2	Isolated
NGC 5953	59	15 34 32.2	15 11 37	13.30	0.00655	Sy2	Interacting
IC 4553	105	15 34 57.1	23 30 07	14.40	0.01812	Sy2	Interacting
IC 5135	30572	21 48 19.5	−34 57 10	13.33	0.01614	Sy2	Isolated
NGC 7682	50588	23 29 03.8	03 31 59	14.30	0.01712	Sy2	Interacting
NGC 7743	40936	23 44 21.3	09 55 56	12.90	0.00440	Sy2	Interacting

Notes. The units of right ascension are hours, minutes and seconds and the units of declination are degrees, arcminutes and arcseconds.

correct Seyfert type classification of our sample. The only special case was the Seyfert galaxy NGC 7172. This object has historically been classified as a Sy2, because of the lack of broad lines in the optical spectrum. However, it has been shown recently that it has a broad component in the Paschen lines (Smajić et al. 2012). Following these authors, we consider this object as an extremely obscured Sy1.

In Table 1 we present the following information: (1) the object names, (2) the *Spitzer* programme identification (PID), (3) and (4) celestial coordinates, (5) *B* magnitudes, (6) redshifts, (7) type of Seyfert and (8) environment of our final list of AGN galaxies with archival low-resolution spectra from the Spitzer IRS.

3 DATA REDUCTION

The IRS observations cover the MIR bandpass from 5.2–38 μm. We downloaded the Basic Calibrated Data (BCDs) with the pipeline version S18.18.0 from the Spitzer Science Center (SSC) and we used the Spitzer IRS Custom Extraction (SPICE) software to extract the spectra. We used the staring-mode observation. The output of SPICE produces one spectrum per order at each nod position; these were combined using an IDL (Interactive Data Language) procedure. For the subtraction of the background sky, we used two nodded observations along the slit of the same order in staring mode, applying standard IRAF routines. We cleaned rogue pixels of the BCDs produced by the *Spitzer* pipeline using the IRSCLEAN software. We scaled the four moduli spectra using the measured flux of the long-wavelength order, which has the widest slit and is the least sensitive to pointing errors. For this purpose we developed an IDL routine, which we also used to combine the spectra and correct the effect of the *14-micron teardrop*. To correct the teardrop, the routine examines the excess in the 13.5–15 μm region, which is due to internal reflection. The correction was needed for the majority of the galaxies in our sample.

4 ANALYSIS

In order to calculate the silicate feature strengths, we measured the continuum over three fitting intervals: the short-wavelength interval

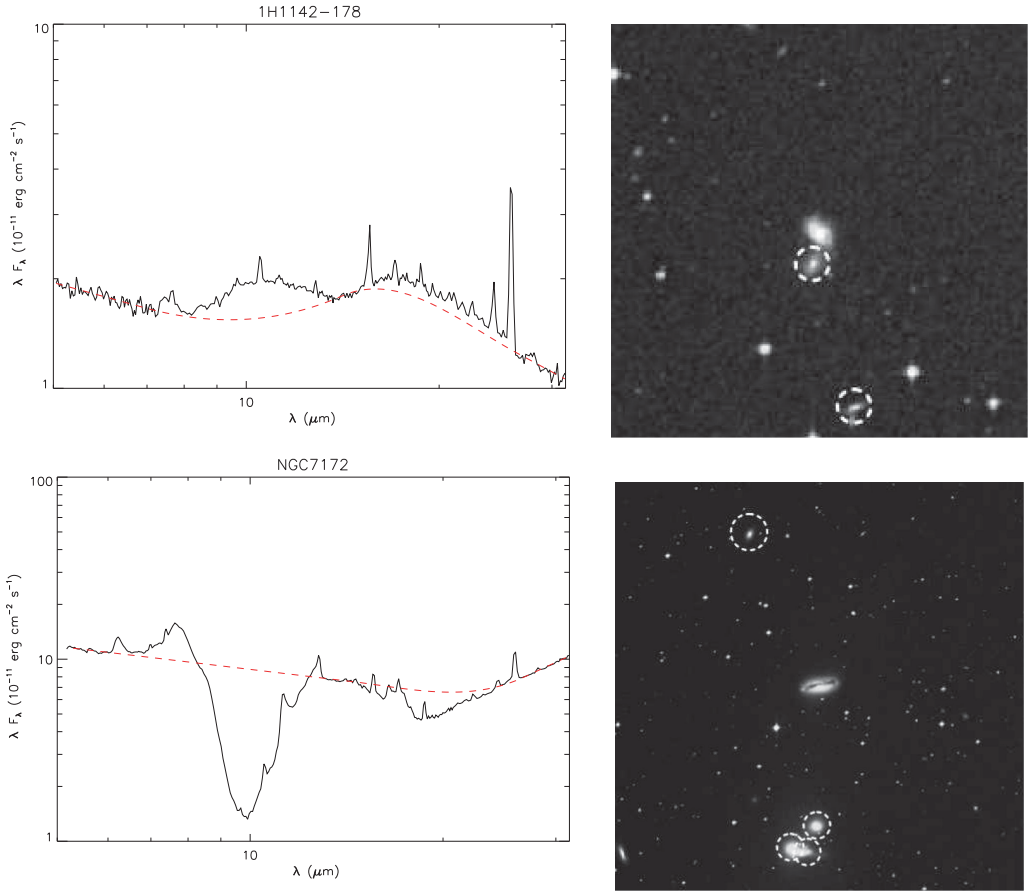

Figure 1. Examples of Sy1 spectra from the Spitzer IRS (black solid lines, left), the continuum-dominated spectrum of 1H1142−178 (top) and the PAH-dominated spectrum of NGC 7172 (bottom). In order to obtain the underlying continuum, we fit a cubic spline (black dashed lines) to measurements over a short-wavelength region, an intermediate interval around 14 μm and a long-wavelength region. Also, this figure shows the NED image of each object (right), with close companions in both cases (white dashed circles).

of 5–7 μm, the intermediate interval (around 14 μm) and the long-wavelength interval of 26.5–31.5 μm. We used a cubic spline in logarithmic space over these fitting regions to determine the full continuum, following the methods suggested by Spoon et al. (2007) and Sirocky et al. (2008). According to these authors, the continuum fitted using a cubic spline resembles within 1 or 2 per cent the emergent continuum spectrum calculated using detailed modelling of synthetic 'featureless dust'. The above intervals are adequate to fit the featureless continuum, since the dust absorption cross-section peaks around 10 and 18 μm (the well-known silicate features produced by dust). The intermediate interval is crucial to obtain a good fit because the cross-section has a local minimum around 14 μm, where the presence of silicate features is negligible (Thompson et al. 2009).

We developed an IDL routine to obtain the continuum fits and silicate strength measurements. We used three different procedures for three different type of spectra: (1) 'continuum-dominated spectra', which show high-ionization emission lines of AGNs and weak PAH emission, (2) 'PAH-dominated spectra', showing strong PAH emission, and (3) 'absorption-dominated' spectra. Following Sirocky et al. (2008), we considered PAH-dominated spectra when the equivalent width in the 6.2-μm band was $EW_{6.2} > 0.05$ μm. The majority of Sy2 galaxies have PAH-dominated spectra (60 per cent), whereas the majority of Sy1 galaxies have continuum-dominated spectra (68 per cent). Our results are in agreement with previous works about the link between type 2 AGNs and higher rates of nuclear star formation inferred by the presence of PAHs (Tielens et al. 2004; Buchanan et al. 2006). We did not find any object with a continuum dominated by absorption.

Fig. 1 shows examples of our fits to the continuum-dominated spectrum of Sy1 galaxy 1H1142−178 and the PAH-dominated spectrum of extremely obscured Sy1 galaxy NGC 7172. Fig. 2 shows the continuum fits for continuum-dominated Sy2 galaxy Mrk 573 and PAH-dominated Sy2 galaxy IC 4553. Both figures show the NED and/or SDSS image of each object. Following (Levenson et al. 2007), we measured the silicate feature strength as

$$S_{\rm sil} = \ln \frac{F_{\rm obs}(\lambda)}{F_{\rm cont}(\lambda)}, \quad (1)$$

where $F_{\rm obs}$ is the observed flux density in the silicate and $F_{\rm cont}$ is the fitted continuum flux density. $F_{\rm obs}$ is based on the local maximum/minimum flux near 10 and 18 μm, where the silicate features are expected. A positive value of the ratio indicates emission and a negative indicates absorption. Table 2 contains silicate feature strengths (S_{10} and S_{18}), peak wavelengths (λ_{10} and λ_{18}) and the dust distribution for our sample. Most Seyfert galaxy spectra show high-excitation lines, such as [O IV] and [Ne V], typical of AGNs (Lutz et al. 2003), as well as low-ionization lines, such as [Ne II] and [S II], which originate in star formation regions. We note that since the [Ne V] emission line is near the intermediate fitting interval around 14 μm, we subtracted this feature before fitting the continuum of this region.

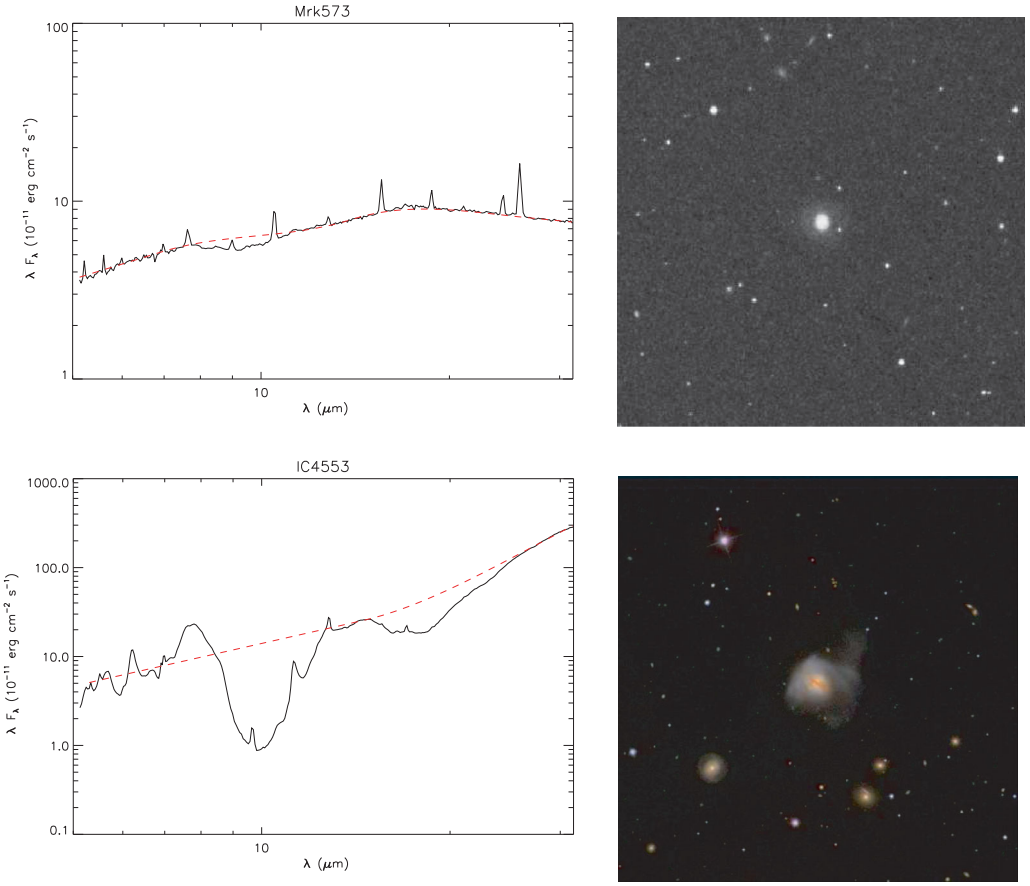

Figure 2. Examples of Sy2 spectra from the Spitzer IRS (black solid lines, left), the continuum-dominated spectrum of Mrk 573 (top) and the PAH-dominated spectrum of IC 4553 (bottom). The continuum fits are denoted by the black dashed lines. Also, this figure shows the NED image of Mrk 573 and SDSS image of IC 4553 (right), with no close companions in both cases.

The main uncertainty in our measurements is the placement of the continuum. However, the error introduced by the uncertainties is small: the systematic differences due to the different assumptions are typically less 10 per cent.

5 RESULTS

For 13 out of 19 Sy1 galaxies, we found the silicate features in emission, albeit weak ($S_{sil} > 0$). Five objects have silicate absorption at 10 μm and emission at 18 μm. The only object showing strong absorption in both features is NGC 7172. As mentioned in Section 2, this is an extremely absorbed object, the broad lines of which are only seen in the NIR. Although the classification of this galaxy might be cumbersome, it does not affect our results. However, we note that this object is in interaction, which may explain the heavy obscuration and deep absorption silicate features (which indicate a smooth dust distribution, see below). Only three out of 17 Sy2s have both silicate features in emission and only three have both features in absorption. Our results are presented in Fig. 3, where the empty symbols correspond to isolated galaxies and the filled symbols to galaxies with one or more companions. In this plot, the triangles identify Seyfert 1, circles mark Seyfert 2, and squares designate Seyfert 1.8 and Seyfert 1.9 AGNs.

The strength of the two silicate features is highly sensitive to the geometric distribution of the dust. Therefore, we used the 'feature–feature' diagram (S_{10} versus S_{18}) proposed by Sirocky et al. (2008) to distinguish smooth distributions from clumpy ones (these two distributions of dust occupy different regions in the silicate feature plane). Fig. 4 presents the dust-distribution diagnostics of the sample. Our results indicate that the clumpy dust-distribution group contains 13 Sy1 and 8 Sy2, while the smooth dust distribution group contains 6 Sy1 and 12 Sy2.

Considering the environment, we find that all of the isolated Sy1 galaxies have clumpy dust geometric distribution, whereas the Sy1s with a close companion can have either clumpy or smooth dust distributions. In the case of Sy2 galaxies, the results are opposite. Those with one or more companions have mostly smooth dust distributions, whereas for those without companions their dust distribution can be either smooth or clumpy. Fig. 5 shows a histogram where the difference in the dust distribution as a function of environment and Seyfert type can be clearly appreciated.

6 DISCUSSION

Based on IRS/*Spitzer* observations, we have found two different circumnuclear dust geometric distributions in our sample of Seyfert galaxies. From Fig. 5, it is clear that Sy2s and Sy1s have somewhat different dust distributions. Overall, Seyfert 1 galaxies tend to have clumpy dust distributions, whereas the dust distributions of Sy2s are more evenly distributed between smooth and clumpy. This result is in agreement with those by Sirocky et al. (2008).

In terms of the environment also, there are striking differences in the dust distributions. Only nine out 23 interacting galaxies have clumpy dust. On the other hand, only four out of 16 isolated Seyferts

Table 2. Spectral measurements.

Galaxy	S_{10}	λ_{10}	S_{18}	λ_{18}	Type	PAH-dominated	Dust distribution
Mrk 590	0.18	10.4	0.08	17.5	Sy1	No	Clumpy
ESO 548−G81	0.31	10.7	0.17	18.0	Sy1	No	Clumpy
NGC 2782	−0.33	9.7	0.20	17.1	Sy1	Yes	Smooth
1H1142−178	0.23	10.7	0.10	17.2	Sy1	No	Clumpy
Mrk 42	−0.08	9.6	0.11	17.2	Sy1	Yes	Clumpy
UGC 7064	−0.20	9.3	0.13	17.1	Sy1	Yes	Smooth
NGC 4235	0.34	12.6	0.24	16.9	Sy1	No	Clumpy
Mrk 50	0.24	10.8	0.37	18.3	Sy1	No	Clumpy
IISZ10	0.21	11.0	0.12	18.6	Sy1	No	Clumpy
NGC 5077	0.22	11.0	0.31	17.1	Sy1	No	Smooth
UM 614	0.17	10.7	0.16	17.2	Sy1	No	Clumpy
Mrk 279	0.14	11.1	0.03	18.3	Sy1	No	Clumpy
NGC 5548	0.14	11.4	0.06	17.2	Sy1	No	Clumpy
Mrk 290	0.20	11.0	0.09	18.1	Sy1	No	Clumpy
NGC 7172	−1.84	9.8	−0.29	18.6	Sy1	Yes	Smooth
Mrk 915	0.05	10.4	0.27	17.1	Sy1	No	Clumpy
UGC 12138	−0.18	9.5	0.14	17.1	Sy1	Yes	Smooth
NGC 7469	-0.16	9.7	0.12	17.2	Sy1	Yes	Smooth
NGC 7603	0.16	11.7	0.13	17.1	Sy1	No	Clumpy
Mrk 744	−0.12	9.7	0.24	17.5	Sy1.8	Yes	Smooth
MCG –03–34–064	−0.22	9.5	0.05	17.0	Sy1.8	No	Clumpy
UGC 1395	−0.34	9.5	0.18	17.2	Sy1.9	Yes	Smooth
NGC 0454	-0.57	9.9	0.06	16.7	Sy2	Yes	Smooth
NGC 526A	0.15	11.3	0.08	18.9	Sy2	No	Clumpy
Mrk 573	−0.10	9.4	0.04	17.2	Sy2	No	Clumpy
NGC 788	−0.08	9.5	0.02	20.5	Sy2	No	Clumpy
IC 1816	−0.42	9.3	0.08	17.2	Sy2	Yes	Smooth
ESO 417−G06	−0.27	9.3	0.18	17.2	Sy2	No	Smooth
NGC 1358	−0.30	9.5	0.00	17.1	Sy2	Yes	Clumpy
NGC 4939	0.30	10.6	0.00	18.0	Sy2	No	Clumpy
NGC 5347	−0.22	9.4	−0.04	18.8	Sy2	No	Clumpy
NGC 5427	−0.12	10.3	0.30	17.6	Sy2	Yes	Smooth
NGC 5506	−0.84	9.8	−0.08	19.5	Sy2	Yes	Smooth
Mrk 686	−0.27	9.73	0.23	17.4	Sy2	No	Smooth
NGC 5953	−0.09	10.1	0.23	17.2	Sy2	Yes	Smooth
IC 4553	−2.78	9.9	−0.87	18.4	Sy2	Yes	Smooth
IC 5135	−0.57	9.8	0.11	17.1	Sy2	Yes	Smooth
NGC 7682	0.05	10.2	0.19	17.2	Sy2	Yes	Clumpy
NGC 7743	−0.29	9.3	0.32	17.1	Sy2	Yes	Smooth

have smooth distributions. Furthermore, there is a clear convolution between the interaction, Seyfert type and dust distribution. This is clear from Fig. 5, where it can be observed that all isolated Sy1 galaxies have clumpy dust distributions, whereas the Sy1s with at least one close companion can equally likely have clumpy or smooth dust distributions. In contrast, two-thirds of Sy2s with one or more close neighbours have smooth distributions, whereas isolated Sy2s have clumpy or smooth dust distributions.

How can the environment influence the dust distribution and the Seyfert type? The presence of a close neighbour may produce a tidal perturbation that in turn may induce a steady inflow of gas and dust into the nuclear region. This flow of material towards the centre will have a smooth dust geometry, which explains why the majority of interacting Seyferts have smooth dust distributions. There are, of course, other possible non-axisymetrical tidal perturbations that can induce such infall. This may explain the fact that some isolated galaxies also have smooth dust distributions.

Our findings can be easily explained in terms of the well-known evolutionary sequence suggested for Seyferts (Krongold et al. 2002, 2003, and references therein) and outlined as follows:

Interaction $\Longrightarrow$ Starburst $\rightarrow$ Seyfert2 $\rightarrow$ Seyfert1.

In this scheme, the interaction is responsible for driving the gas towards the centre and this infall ignites star formation activity (Ellison et al. 2010) and feeds the supermassive black hole. At this stage, the dust covering factor of the AGN is nearly 1 and a smooth dust distribution is expected. As the starburst dies off, an initial composite Seyfert 2 + starburst nucleus evolves into an obscured Seyfert galaxy, which could be seen as Sy1 or Sy2 depending on the covering factor of the dust torus as well as the orientation (assuming there is indeed a broad-line region, which is not always the case). The nucleus would be observed with an older stellar population (Boisson et al. 2000). Thus, in this scenario, inclination/obscuration effects are indeed present, but only during the last phase of the above evolutionary sequence (see also Koulouridis et al. 2006a, 2007). The scenario is further supported by other works, which show that recent circumnuclear star-forming regions are present more frequently in type 2 than in type 1 AGNs (Maiolino et al. 1997; Gu et al. 2001; Coldwell et al. 2009). Recent studies by Castro et al. (2014) also support it, at least for low-luminosity AGNs. The sequence has also been observed for low-ionization nuclear emission-line region galaxies (LINERs) (Krongold et al. 2003), ultraluminous infrared galaxies (ULIRGs) and quasars (e.g. Haas et al. 2003; Fiore et al. 2008), suggesting

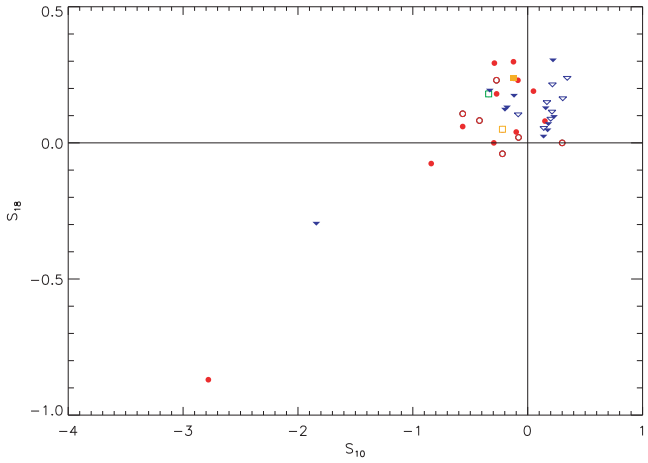

Figure 3. Measured strengths of the 10- and 18-μm silicate features (S_{10} versus S_{18}). For 13 out of 19 Sy1 galaxies, we found the silicate features in emission, albeit weak ($S_{\rm sil} > 0$). Only three out of 17 Sy2s have both silicate features in emission and only three have both features in absorption. Positive strength indicates emission ($S_{\rm sil} > 0$) and negative strength indicates absorption ($S_{\rm sil} < 0$). The triangles identify Seyfert 1, circles mark Seyfert 2, and squares designate Seyfert 1.8 and Seyfert 1.9 AGNs. The empty symbols are isolated galaxies and the fill symbols are galaxies with one or more companions.

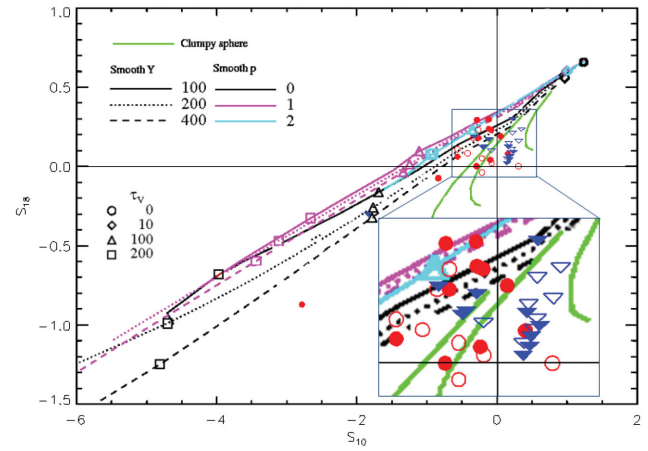

Figure 4. The 'feature–feature' diagnostic diagram of our Seyfert galaxies sample. This diagram shows the numerical simulation of silicate feature strengths around 10 and 18 μm using a spherical shell distribution of dust, cool and oxygen-rich silicates (OHMc) (Ossenkopf, Henning & Mathis 1992), computed by Sirocky et al. (2008). For clumpy models, each track represents the mean number of clouds N_0 along the line of sight ($N_0 = 1$, 3 and 5 from upper right to lower left, respectively), with $Y = 30$, which is the shell thickness, and $p = 0$, where the radial density profile is proportional to r^{-p}. For smooth models, the line style shows different shell thickness, Y, and the colour shows the radial density profile, p. Black open symbols indicate total optical depth $\tau_{\rm v}$. For our sample of galaxies, we used triangles to identify Seyfert 1 AGNs and circles to identify Seyfert 2 AGNs. The empty symbols are isolated galaxies and the fill symbols are galaxies with one or more companions.

that it is luminosity-independent. Further evidence in favour of this sequence is found in Villarroel, Korn & Matsuoka (2012), Kollatschny, Reichstein & Zetzl (2012) and Koulouridis et al. (2013). The evolutionary scheme can also explain the high frequency of starbursts and Sy 2 nuclei observed in close interacting systems, as well as the lack of type 1 nuclei (e.g. González et al. 2008) for interacting pairs and compact groups (Martínez et al. 2008; Bitsakis et al. 2010).

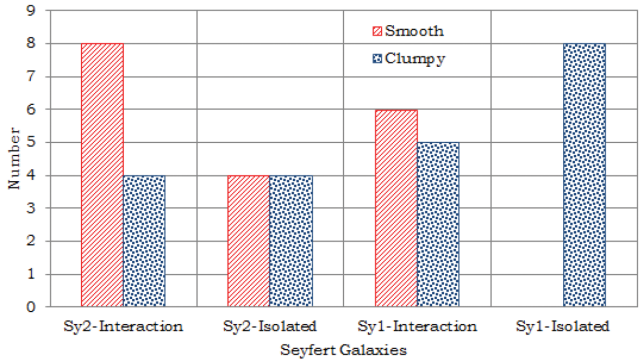

Figure 5. Histogram of our sample of Seyfert galaxies in interaction and non-interaction and their geometric distribution of dust. From this histogram it is clear that all of the isolated Sy1 galaxies have clumpy dust distributions, whereas the Sy1s with at least one close companion can have either clumpy or smooth dust distributions. In contrast, two-thirds of Sy2s with one or more close neighbours have smooth distributions, whereas isolated Sy2s have equal numbers of clumpy or smooth dust distributions.

The torus covering factor changes along the proposed evolutionary sequence. In the early stages, if an AGN exists, it is obscured from all or most lines of sight. As the SB evolves, the dust inflow decreases, its distribution flattens (Haas et al. 2003) so that more of the sky – as seen from the central engine – is uncovered and the covering factor diminishes. Thus the probability of detecting the AGN increases over time.

According to Elitzur (2012), increased clumpiness of the dust over time would enable this, because when the dust distribution becomes more patchy it becomes easier to detect the AGN. This 'realistic unification' (Elitzur 2012) takes the clumpiness of the torus into account and suggests that there is a smooth distribution in its covering factor. Type 2 AGN are more likely to be drawn from the higher end distribution of the dust covering factor and this suggestion has received some observational support (e.g. Ramos Almeida et al. 2009, 2011).

Our evolutionary scenario is compatible with this 'realistic unification'. At early stages, most objects will be type 2s and the probability of observing the interacting neighbour is high. Then both types 1 and 2 may be found, depending on orientation ('unification stage'). At the later stage, we see mostly type 1 objects, because it becomes easier to detect the BLR. Also at this later stage, the probability of seeing the companion has diminished, because the companion has either fled away or merged, leaving no trace of the process.

7 CONCLUSION

We have analysed a sample of Sy1 and Sy2 galaxies, both isolated and in interaction, observed by *Spitzer*. We found that all of the isolated Sy1s have clumpy dust distributions, while the interacting Sy1s have both clumpy and smooth dust distributions. On the other hand, the dust distributions of isolated Sy2s can be either smooth or clumpy, whereas the majority of interacting Sy2s have smooth dust distributions. This indicates a connection between the presence of a close companion and the distribution of the circumnuclear dust in Seyfert galaxies. These findings can easily be explained in the context of an evolutionary sequence for Seyfert galaxies (Krongold et al. 2002, 2003), as explained in the discussion. This sequence is also observed at higher luminosities (Sanders et al. 1988a,b; Haas et al. 2003; Fiore et al. 2008), from mergers to ULIRGs to quasars,

and suggests that the dust distribution is strongly influenced by gravitational interactions.

ACKNOWLEDGEMENTS

SMC acknowledges a graduate student scholarship from CONACYT. DD acknowledges support from grant IN107313 from PAPIIT, UNAM. This work is based on observations made with the Spitzer*Space Telescope* and has made use of the NASA/IPAC Extragalactic Database, both of which are operated by the Jet Propulsion Laboratory, California Institute of Technology, under contracts with NASA. Funding for the SDSS and SDSS-II has been provided by the Alfred P. Sloan Foundation, the Participating Institutions, the National Science Foundation, the U.S. Department of Energy, the National Aeronautics and Space Administration, the Japanese Monbukagakusho, the Max Planck Society, and the Higher Education Funding Council for England. The SDSS Web Site is http://www.sdss.org/.

The SDSS is managed by the Astrophysical Research Consortium for the Participating Institutions. The Participating Institutions are the American Museum of Natural History, Astrophysical Institute Potsdam, University of Basel, University of Cambridge, Case Western Reserve University, University of Chicago, Drexel University, Fermilab, the Institute for Advanced Study, the Japan Participation Group, Johns Hopkins University, the Joint Institute for Nuclear Astrophysics, the Kavli Institute for Particle Astrophysics and Cosmology, the Korean Scientist Group, the Chinese Academy of Sciences (LAMOST), Los Alamos National Laboratory, the Max-Planck-Institute for Astronomy (MPIA), the Max-Planck-Institute for Astrophysics (MPA), New Mexico State University, Ohio State University, University of Pittsburgh, University of Portsmouth, Princeton University, the United States Naval Observatory, and the University of Washington.

REFERENCES

Antonucci R., 1993, ARA&A, 31, 473
Antonucci R. R. J., Miller J. S., 1985, ApJ, 297, 621
Bianchi S., Corral A., Panessa F., Barcons X., Matt G., Bassani L., Carrera F. J., Jiménez-Bailón E., 2008, MNRAS, 385, 195
Bitsakis T., Charmandaris V., Le Floc'h E., Díaz-Santos T., Slater S. K., Xilouris E., Haynes M. P., 2010, A&A, 517, A75
Boisson C., Joly M., Moultaka J., Pelat D., Serote Roos M., 2000, A&A, 357, 850
Brightman M., Nandra K., 2008, MNRAS, 390, 1241
Buchanan C. L., Gallimore J. F., O'Dea C. P., Baum S. A., Axon D. J., Robinson A., Elitzur M., Elvis M., 2006, AJ, 132, 401
Cid Fernandes R., Heckman T., Schmitt H., González Delgado R. M., Storchi-Bergmann T., 2001, ApJ, 558, 81
Coldwell G. V., Lambas D. G., Söchting I. K., Gurovich S., 2009, MNRAS, 399, 88
Dultzin-Hacyan D., Benitez E., 1994, A&A, 291, 720
Dultzin-Hacyan D., Ruano C., 1996, A&A, 305, 719
Dultzin-Hacyan D., Krongold Y., Fuentes-Guridi I., Marziani P., 1999, ApJ, 513, L111
Efstathiou A., Rowan-Robinson M., 1995, MNRAS, 273, 649
Elitzur M., 2008, Mem. Soc. Astron. Ital., 79, 1124
Elitzur M., 2012, ApJ, 747, LL33
Ellison S. L., Patton D. R., Simard L., McConnachie A. W., Baldry I. K., Mendel J. T., 2010, MNRAS, 407, 1514
Fiore F. et al., 2008, ApJ, 672, 94
González J. J., Krongold Y., Dultzin D., Hernández-Toledo H. M., Huerta E. M., Olguín L., Marziani P., Cruz-González I., 2008, Revista Mexicana de Astronomia y Astrofisica Conference Series, 32, 170
Gonzalez-Delgado R. M., Perez E., 1993, Ap&SS, 205, 127
Granato G. L., Danese L., 1994, MNRAS, 268, 235
Gu Q., Maiolino R., Dultzin-Hacyan D., 2001, A&A, 366, 765
Haas M. et al., 2003, A&A, 402, 87
Houck J. R. et al., 2004, ApJS, 154, 18
Imanishi M., Wada K., 2004, ApJ, 617, 214
Knacke R. F., Thomson R. K., 1973, PASP, 85, 341
Kollatschny W., Reichstein A., Zetzl M., 2012, A&A, 548, A37
Koulouridis E., Plionis M., Chavushyan V., Dultzin-Hacyan D., Krongold Y., Goudis C., 2006a, ApJ, 639, 37
Koulouridis E., Chavushyan V., Plionis M., Krongold Y., Dultzin-Hacyan D., 2006b, ApJ, 651, 93
Koulouridis E., Plionis M., Chavushyan V., Dultzin-Hacyan D., Krongold Y., Goudis C., 2007, ApJ, 657, 642
Koulouridis E., Plionis M., Chavushyan V., Dultzin D., Krongold Y., Georgantopoulos I., León-Tavares J., 2013, A&A, 552, A135
Krolik J. H., Begelman M. C., 1988, ApJ, 329, 702
Krongold Y., Dultzin-Hacyan D., Marziani P., 2002, ApJ, 572, 169
Krongold Y., Dultzin-Hacyan D., Marziani P., de Diego J. A., 2003, Rev. Mex. Astron. Astrofis., 39, 225
Levenson N. A., Sirocky M. M., Hao L., Spoon H. W. W., Marshall J. A., Elitzur M., Houck J. R., 2007, ApJ, 654, L45
Lipovetsky V. A., Neizvestny S. I., Neizvestnaya O. M., 1988, Soobshcheniya Spetsial'noj Astrofizicheskoj Observatorii, 55, 5
Lutz D., Sturm E., Genzel R., Spoon H. W. W., Moorwood A. F. M., Netzer H., Sternberg A., 2003, A&A, 409, 867
Maiolino R., Rieke G. H., 1995, ApJ, 454, 95
Maiolino R., Ruiz M., Rieke G. H., Papadopoulos P., 1997, ApJ, 485, 552
Martínez M. A., Del Olmo A., Coziol R., Perea J., 2008, Revista Mexicana de Astronomia y Astrofisica Conference Series, 32, 164
Marzke R. O., Geller M. J., da Costa L. N., Huchra J. P., 1995, AJ, 110, 477
Nenkova M., Ivezić Ž., Elitzur M., 2002, ApJ, 570, L9
Nenkova M., Sirocky M. M., Ivezić Ž., Elitzur M., 2008a, ApJ, 685, 147
Nenkova M., Sirocky M. M., Nikutta R., Ivezić Ž., Elitzur M., 2008b, ApJ, 685, 160
Nicastro F., 2000, ApJ, 530, L65
Ossenkopf V., Henning T., Mathis J. S., 1992, A&A, 261, 567
Pier E. A., Krolik J. H., 1992, ApJ, 401, 99
Pier E. A., Krolik J. H., 1993, ApJ, 418, 673
Ramos Almeida C. et al., 2009, ApJ, 702, 1127
Ramos Almeida C. et al., 2011, ApJ, 731, 92
Rowan-Robinson M., 1995, MNRAS, 272, 737
Sanders D. B., Soifer B. T., Elias J. H., Madore B. F., Matthews K., Neugebauer G., Scoville N. Z., 1988a, ApJ, 325, 74
Sanders D. B., Soifer B. T., Elias J. H., Neugebauer G., Matthews K., 1988b, ApJ, 328, L35
Shu X.-W., Wang J.-X., Jiang P., 2008, Chin. J. Astron. Astrophys., 8, 204
Sirocky M. M., Levenson N. A., Elitzur M., Spoon H. W. W., Armus L., 2008, ApJ, 678, 729
Smajić S., Fischer S., Zuther J., Eckart A., 2012, A&A, 544, A105
Spoon H. W. W., Marshall J. A., Houck J. R., Elitzur M., Hao L., Armus L., Brandl B. R., Charmandaris V., 2007, ApJ, 654, L49
Thompson G. D., Levenson N. A., Uddin S. A., Sirocky M. M., 2009, ApJ, 697, 182
Tielens A. G. G. M., Peeters E., Bakes E. L. O., Spoon H. W. W., Hony S., 2004, in Johnstone D., Adams F. C., Lin D. N. C., Neufeld D. A., Ostriker E. C., eds, ASP Conf. Proc. Vol. 323, Star Formation in the Interstellar Medium: In Honor of David Hollenbach, Chris McKee and Frank Shu. Astron. Soc. Pac., San Francisco, p. 135
Torres-Flores S., de Oliveira C. M., de Mello D. F., Scarano S., Urrutia-Viscarra F., 2012, MNRAS, 421, 3612
Tran H. D., 2001, ApJ, 554, L19
Tran H. D., 2003, ApJ, 583, 632
Villarroel B., Korn A., Matsuoka Y., 2012, preprint (arXiv:1211.0528)
Werner M. W. et al., 2004, ApJS, 154, 1

This paper has been typeset from a TEX/LATEX file prepared by the author.